Journal of Sound and Vibration (1999) **226**(2), 329–344
Article No. jsvi.1999.2300, available online at http://www.idealibrary.com on IDEAL®

STATISTICAL THEORY OF THE VECTOR RANDOM DECREMENT TECHNIQUE

J. C. ASMUSSEN AND R. BRINCKER

Department of Building Technology and Structural Engineering, Aalborg University, Denmark

AND

S. R. IBRAHIM

Department of Mechanical Engineering, Old Dominion University, Virginia, U.S.A.

(*Received* 27 *February* 1998, *and in final form* 7 *April* 1999)

The Vector Random Decrement technique has previously been introduced as an efficient method to transform ambient responses of linear structures into Vector Random Decrement functions which are equivalent to free decays of the current structure. The modal parameters can be extracted from the free decays. Due to the speed and/or accuracy of the Vector Random Decrement technique, it was introduced as an attractive alternative to the Random Decrement technique. In this paper, the theory of the Vector Random Decrement technique is extended by applying a statistical description of the stochastic processes describing the ambient measurements. The Vector Random Decrement functions are linked to the correlation functions of the stochastic processes provided they are stationary and Gaussian distributed. Furthermore, a new approach for quality assessment of the Vector Random Decrement functions is given on the basis of the derived results. The work presented in this paper makes the theory of the Vector Random Decrement technique equivalent to the theory of the Random Decrement technique. The theoretical derivations are illustrated by the analysis of the response of a 3DOF system loaded by white noise.

1. INTRODUCTION

Assignments such as, for example updating of a theoretical model, force identification or inspection and reliability evaluation motivate the performance of vibration testing of large structures. Usually, the purpose of a vibration test is to estimate the modal parameters of the structure, which can then be used for further analysis of the dynamic behaviour of the structure. This indirectly assumes that the vibrations at the measurement points of the structure can be modelled by a viscously damped linear lumped mass parameter system of finite size

$$\mathbf{M}\ddot{\mathbf{X}}(t) + \mathbf{C}\dot{\mathbf{X}}(t) + \mathbf{K}\mathbf{X}(t) = \mathbf{F}(t), \tag{1}$$

0022-460X/99/370329 + 16 $30.00/0

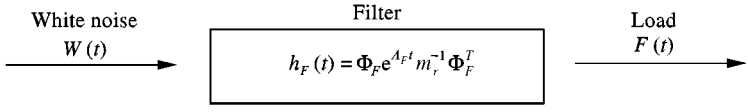

Figure 1. Outline diagram for modelling of loads by using a shaping filter. $h(t)$ is the impulse response matrix. Φ_F contains the mode shapes of the filter. Λ_F contains the eigenvalues and m_F is a normalizing matrix.

where **M**, **C** and **K** are the square mass, damping and stiffness matrices of size n. $\mathbf{X}(t)$ is the stochastic response vector to the stochastic load vector $\mathbf{F}(t)$ both of size $n \times 1$.

In testing of large structures, such as bridges, ambient excitation (traffic, wind, micro-tremors, etc) is very attractive, since it does not require that the structure is taken out of service. The unmeasurable ambient forces are modelled mathematically as white noise excitation at the lumped masses of the mathematical model of the structure; see equation (1). In order to make the force modelling more versatile it can be generalized to white noise passed through a linear shaping filter, see reference [1, 2].

The mathematical modelling of the ambient forces makes the theory equivalent to the situation where the structure has been excited by artifical white noise applied by a shaker.

If the structure and the forces can be modelled as described above it is well known that the correlation functions $\mathbf{R}_{\mathbf{XX}}(\tau)$ of the measurements $\mathbf{X}(t)$ are equivalent to the response of the structure to initial conditions only; see, e.g. references [2–4]. The ith column in the correlation matrix, $\mathbf{R}_{\mathbf{X}_i}(\tau)$ is given by

$$\mathbf{R}_{\mathbf{X}_i}(\tau) = \bar{\mathbf{\Phi}} e^{\bar{\Lambda}\tau} \mathbf{C}_i, \quad \tau > 0, \tag{2}$$

where $\bar{\mathbf{\Phi}}$ is the mode shape matrix with the mode shapes of the structure and the filter, $\bar{\mathbf{\Lambda}}$ is a diagonal matrix with the eigenvalues of the structure and the filter. The $\mathbf{C}_i$ vector can be interpreted as a weighting vector or an initial condition vector, which depends on $\bar{\mathbf{\Phi}}$, $\bar{\mathbf{\Lambda}}$, the modal masses of the structure and the filter and the covariance matrix of the white noise process $\mathbf{W}(t)$.

The effect of the force shaping filter is that it is not necessary to assume that the forces are white noise. The filter can shape the force spectral density to be non-flat and thereby introduce correlation. The consequence is that the mathematical modes used to model the shape of the spectral density of the force are present in the correlation functions of the responses.

If the correlation functions of the responses are estimated, the results of equation (2) state that the modal parameters of the structure and the force modelling can be extracted by using well-known methods like Polyreference Time Domain technique, Ibrahim Time Domain technique, Auto-Regressive Vector models, etc. These methods are developed to extract modal parameters from the free responses of linear lumped mass parameter systems.

The correlation functions can be estimated by using several different algorithms such as for example the direct approach or an unbiased FFT-IFFT approach, see reference [5]. Another algorithm is the Random Decrement (RD) technique. This

algorithm has recently been applied to ambient measurements [6–11]. The main advantage of the RD technique is the speed [19, 20].

The auto, $D_{XX}(\tau)$, $D_{YY}(\tau)$ and cross, $D_{YX}(\tau)$ $D_{XY}(\tau)$, RD functions of two stationary stochastic processes, $X(t)$ and $Y(t)$ are defined as conditional mean values,

$$D_{XX}(\tau) = E[X(t+\tau)|\, T_{X(t)}], \quad D_{XY}(\tau) = E[X(t+\tau)|\, T_{Y(t)}],$$

$$D_{YX}(\tau) = E[Y(t+\tau)|\, T_{X(t)}], \quad D_{YY}(\tau) = E[Y(t+\tau)|\, T_{Y(t)}], \tag{3}$$

where $T_{X(t)}$ denotes the triggering condition, which in the most general case can be formulated as the applied general triggering condition, $T^{G_A}_{X(t)}$,

$$T^{G_A}_{X(t)} = \{a_1 \leqslant X(t) < a_2, b_1 \leqslant \dot{X}(t) < b_2\}. \tag{4}$$

All specific triggering conditions can be formulated from $T^{G_A}_{X(t)}$. In application to ambient testing, the banded positive triggering condition $T^{P}_{X(t)}$, is usually applied:

$$T^{P}_{X(t)} = \{a_1 \leqslant X(t) < a_2\}. \tag{5}$$

The RD functions are estimated as empirical mean values,

$$\hat{D}_{XX}(\tau) = \frac{1}{N}\sum_{i=1}^{N} x(t_i+\tau)|\, T_{x(t_i)}, \quad \hat{D}_{XY}(\tau) = \frac{1}{N}\sum_{i=1}^{N} x(t_i+\tau)|\, T_{y(t_i)},$$

$$\hat{D}_{YX}(\tau) = \frac{1}{N}\sum_{i=1}^{N} y(t_i+\tau)|\, T_{x(t_i)}, \quad \hat{D}_{YY}(\tau) = \frac{1}{N}\sum_{i=1}^{N} y(t_i+\tau)|\, T_{y(t_i)}, \tag{6}$$

which assumes that the stochastic processes are ergodic. $x(t)$ and $y(t)$ are realizations of $X(t)$ and $Y(t)$ and N denotes the number of triggering points. N depends not only on the length of the realizations, but also on the choice of a_1, a_2 and b_1, b_2.

The RD technique was introduced [12–15] as a method to transfer the random response of a SDOF system to the free decays of the SDOF system. Later the RD technique was extended to multiple measurements/multiple modes by introduction of equation (6) in combination with the ITD algorithm [16, 17]. The theoretical background of the RD technique was extended by linking the RD functions to correlation functions [18, 19, 2]. If the processes $X(t)$ and $Y(t)$ are Gaussian distributed, the following relation holds for the applied general triggering condition [19, 2]:

$$D_{XX}(\tau) = \frac{R_{XX}(\tau)}{\sigma_X^2}\,\tilde{a}_X - \frac{R'_{XX}(\tau)}{\sigma_{\dot{X}}^2}\,\tilde{b}_{\dot{X}}, \quad D_{XY}(\tau) = \frac{R_{XY}(\tau)}{\sigma_Y^2}\,\tilde{a}_Y - \frac{R'_{XY}(\tau)}{\sigma_{\dot{Y}}^2}\,\tilde{b}_{\dot{Y}},$$

$$D_{YX}(\tau) = \frac{R_{YX}(\tau)}{\sigma_X^2}\,\tilde{a}_X - \frac{R'_{YX}(\tau)}{\sigma_{\dot{X}}^2}\,\tilde{b}_{\dot{X}}, \quad D_{YY}(\tau) = \frac{R_{YY}(\tau)}{\sigma_Y^2}\,\tilde{a}_Y - \frac{R'_{YY}(\tau)}{\sigma_{\dot{Y}}^2}\,\tilde{b}_{\dot{Y}}, \tag{7}$$

Here R_{XX}, R_{YY} are autocorrelation functions, R_{YX} and R_{XY} are cross-correlation functions, R' denotes the time derivative of R, σ_X, σ_Y are standard deviations of

X and Y, $\sigma_{\dot{X}}, \sigma_{\dot{Y}}$ are standard deviations of the time derivative of X and Y, respectively, and

$$\tilde{a}_X = \frac{\int_{a_1}^{a_2} x p_X(x)\,\mathrm{d}x}{\int_{a_1}^{a_2} p_X(x)\,\mathrm{d}x}, \quad \tilde{a}_Y = \frac{\int_{a_1}^{a_2} y p_Y(y)\,\mathrm{d}y}{\int_{a_1}^{a_2} p_Y(y)\,\mathrm{d}y},$$

$$\tilde{b}_{\dot{X}} = \frac{\int_{a_1}^{a_2} \dot{x} p_{\dot{X}}(\dot{x})\,\mathrm{d}\dot{x}}{\int_{a_1}^{a_2} p_{\dot{X}}(\dot{x})\,\mathrm{d}\dot{x}}, \quad \tilde{b}_{\dot{Y}} = \frac{\int_{a_1}^{a_2} \dot{y} p_{\dot{Y}}(\dot{y})\,\mathrm{d}\dot{y}}{\int_{a_1}^{a_2} p_{\dot{Y}}(\dot{y})\,\mathrm{d}\dot{y}}, \tag{8}$$

where for example $p_X(x)$ denotes the density function of X. The results of the RD technique under the above modelling of the structure and the loads are parallel to the results of applying the FFT algorithm, because the RD functions are proportional to the correlation functions of the responses.

The advantages of the RD technique are the simple and fast estimation algorithm compared to the FFT algorithm. Results of simulation studies [19, 20] indicate that the RD technique is faster than an unbiased FFT-IFFT approach. Furthermore, the RD technique provides unbiased estimates of the correlation functions [2].

No matter which approach is used to estimate correlation functions, problems arise in the analysis of several simultaneously recorded measurements. The problem is that if n measurements are used, n columns with n correlation functions can be estimated. If n is a large number it becomes computationally difficult to estimate a full correlation matrix corresponding to n^2 correlation functions. Instead only a single or a few columns of the correlation matrix could be estimated. But this opens another problem, because the columns of the correlation matrix have to be chosen carefully. Not all modes will necessarily be properly represented in all columns and also the signal-to-noise ratio of the measurements should be taken into consideration. If a measurement is known to have a high content of noise, the measurement should only be used for averaging and not as a triggering measurement.

These problems motivated the development of the Vector Random Decrement (VRD) technique [21–23] as a computationally efficient method to transfer random responses to free responses.The difference between the RD and the VRD technique is that for the VRD technique the triggering condition is a vector condition. In references [21, 22] the theory which links the VRD functions to the free responses of the measurements is given.

The main issue of this paper is to present a theoretical proof for the relation between the VRD functions and the correlation functions of the stochastic processes describing the collected measurements. This means that the VRD technique theoretically becomes as well described as the RD technique. In section 2, the VRD functions are defined and the different possibilities for the formulation of the technique are described. It is shown that the VRD technique can be considered to be a generalization of the RD technique. In section 3, the theoretical proof for the

link between the VRD functions and the correlation functions is given. In section 4, a simple example which illustrates the advantages of the VRD technique compared to the traditional methods for estimation of correlation function is given. The paper is finished with a conclusion.

2. DEFINITION OF VRD FUNCTIONS

Consider a stationary stochastic vector process $\mathbf{X}(t) = [X_1(t)X_2(t)X_3(t) \ldots X_{k-1}(t)X_k(t)\ X_{k+1}(t) \ldots X_{l-1}X_l(t)X_{l+1}(t) \ldots X_n(t)]^{\mathrm{T}}$, $l > k$. The VRD functions are defined as the conditional mean value of the process $\mathbf{X}(t)$,

$$\mathbf{D}_{\mathbf{XX}_{k,l}}(\tau) = E[\mathbf{X}(t+\tau) | T^v_{\mathbf{X}_{k,l}(t+\Delta\mathbf{t})}], \tag{9}$$

where τ is the time variable of the VRD functions defined for both positive and negative time and $T^v_{\mathbf{X}_{k,l}(t+\Delta t)}$ is the vector triggering condition given by

$$T^v_{\mathbf{X}_{k,l}(t+\Delta\mathbf{t})} = T^v_{X_k(t+\Delta t_k), X_{k+1}(t+\Delta t_{k+1}), \ldots, X_l(t+\Delta t_l)}, \quad 2 \leqslant k < l \leqslant n. \tag{10}$$

The size of the vector triggering condition is by definition greater than or equal to two. If there only is one condition the original formulation for the RD technique is obtained. Physically, a vector triggering condition can be interpreted as a vector which forces the responses to have certain well-defined initial conditions before time segments are picked out and averaged. The VRD technique differs from the RD technique not only by the size of the condition but also by the time shifts introduced to the conditions at the individual elements of the vector process $\mathbf{X}(t)$. The time shifts are introduced in order to make the vector triggering condition more versatile. The exact formulation of $T^v_{\mathbf{X}_{k,l}(t+\Delta\mathbf{t})}$ is discussed in section 3.

By assuming that $\mathbf{X}(t)$ is ergodic, the VRD functions can be estimated from a single realization of $\mathbf{X}(t)$,

$$\hat{\mathbf{D}}_{\mathbf{XX}_{k,l}}(\tau) = \frac{1}{N}\sum_{i=1}^{N} \mathbf{x}(t_i+\tau) | T^v_{\mathbf{x}_{k,l}(t_i+\Delta\mathbf{t})}, \tag{11}$$

where $\mathbf{x}(t)$ is a realization of $\mathbf{X}(t)$. The estimation of the VRD functions is unbiased:

$$E[\hat{\mathbf{D}}_{\mathbf{XX}_{k,l}}(\tau)] = \frac{1}{N}\sum_{i=1}^{N} E[\mathbf{X}(t_i+\tau) | T^v_{\mathbf{X}_{k,l}(t_i+\Delta\mathbf{t})}] = \mathbf{D}_{\mathbf{XX}_{k,l}}(\tau). \tag{12}$$

In the formulation of $T^v_{\mathbf{X}_{k,l}(t+\Delta\mathbf{t})}$ it is important to take into account that the estimation using equation (11) should contain sufficient triggering points so that the estimate converges to the mean value.

In order to illustrate the VRD technique, the following stationary stochastic vector process is considered: $\mathbf{X}(t) = [X_1(t)X_2(t)X_3(t)X_4(t)X_5(t)X_6(t)X_7(t)X_8(t)]$. Four different sets of VRD functions could be defined by the following triggering conditions:

$$\begin{aligned} T^v_{\mathbf{X}_{1,2}(t+\Delta\mathbf{t})} &= T^v_{X_1(t+\Delta t_1), X_2(t+\Delta t_2)}, \quad T^v_{\mathbf{X}_{3,4}(t+\Delta\mathbf{t})} = T^v_{\mathbf{X}_3(t+\Delta t_3), X_4(t+\Delta t_4)}, \\ T^v_{\mathbf{X}_{5,6}(t+\Delta\mathbf{t})} &= T^v_{X_5(t+\Delta t_5), X_6(t+\Delta t_5)}, \quad T^v_{\mathbf{X}_{7,8}(t+\Delta\mathbf{t})} = T^v_{\mathbf{X}_7(t+\Delta t_7), X_8(t+\Delta t_8)}. \end{aligned} \tag{13}$$

Alternatively, only two sets of VRD functions could be defined by using the following triggering conditions:

$$T^{v}_{\mathbf{X}_{1,5}(t+\boldsymbol{\Delta t})} = T^{v}_{X_1(t+\Delta t_1), X_2(t+\Delta t_2), X_3(t+\Delta t_3), X_4(t+\Delta t_4), X_5(t+\Delta t_5)},$$

$$T^{v}_{\mathbf{X}_{6,8}(t+\boldsymbol{\Delta t})} = T^{v}_{X_6(t+\Delta t_6), X_7(t+\Delta t_7), X_8(t+\Delta t_8)}. \tag{14}$$

Here the vector sizes 3 and 5 have been used instead of 4 and 4 for illustration purposes. This example shows how versatile the VRD technique is, since the vector size of the triggering condition can be chosen in several different ways.

3. STATISTICAL THEORY OF THE VRD TECHNIQUE

The stationary stochastic vector process $\mathbf{X}(t)$ defined in section 2 is considered again. It is furthermore assumed that $\mathbf{X}(t)$ is zero mean Gaussian distributed. The correlation matrix of $\mathbf{X}(t)$ at any time difference τ is defined as

$$\mathbf{R}_{\mathbf{XX}}(\tau) = E[\mathbf{X}(t+\tau)\mathbf{X}(t)^{\mathrm{T}}]$$

$$= \begin{bmatrix} R_{X_1X_1(\tau)} & R_{X_1X_2(\tau)} & \cdots & R_{X_1X_n(\tau)} \\ R_{X_2X_1(\tau)} & R_{X_2X_2(\tau)} & \cdots & R_{X_1X_n(\tau)} \\ \vdots & \vdots & \vdots & \\ R_{X_nX_1(\tau)} & R_{X_nX_2(\tau)} & \cdots & R_{X_nX_n(\tau)} \end{bmatrix}, \tag{15}$$

which for simplicity can be rewritten as

$$\mathbf{R}_{\mathbf{XX}}(\tau) = [\mathbf{R}_{X_1}\ \mathbf{R}_{X_2} \cdots \mathbf{R}_{X_k} \cdots \mathbf{R}_{X_t} \cdots \mathbf{R}_{X_n}], \tag{16}$$

where

$$\mathbf{R}_{\mathbf{X}_i} = [R_{X_1X_i}\ R_{X_2X_i} \cdots R_{X_kX_i} \cdots R_{X_lX_i} \cdots R_{X_nX_i}]^{\mathrm{T}}. \tag{17}$$

To develop the theory of the VRD technique, two stochastic vector processes, $\mathbf{X}_v(t)$ and $\mathbf{Y}_v(\mathbf{t})$ which both are contained in $\mathbf{X}(t)$, are considered:

$$\mathbf{X}_v(t) = \begin{bmatrix} X_1(t+\tau) \\ X_2(t+\tau) \\ \vdots \\ X_k(t+\tau) \\ X_{k+1}(t+\tau) \\ \vdots \\ X_l(t+\tau) \\ \vdots \\ X_n(t+\tau) \end{bmatrix}, \quad \mathbf{Y}_v(t) = \begin{bmatrix} X_k(t+\Delta t_k) \\ X_{k+1}(t+\Delta t_{k+1}) \\ \vdots \\ X_l(t+\Delta t_l) \end{bmatrix}. \tag{18}$$

Here $X_i(\cdot)$ refers to the elements of the vector process $\mathbf{X}(t)$. The time shifts Δt_i could be both positive and negative. The size of the stochastic vector proces $\mathbf{Y}_v(t)$ is restricted to be smaller than or equal to the size of $\mathbf{X}_v(t)$. The auto correlation matrix of $\mathbf{Y}_v$ at the time lag zero is given by

$$\mathbf{R}_{\mathbf{Y}_v\mathbf{Y}_v} = E[\mathbf{Y}_v(t)\mathbf{Y}_v^{\mathrm{T}}(t)]$$

$$= \begin{bmatrix} R_{X_kX_k}(0) & R_{X_kX_{k+1}}(\Delta t_k - \Delta t_{k+1}) & \cdots & R_{X_kX_l}(\Delta t_k - \Delta t_l) \\ R_{X_{k+1}X_k}(\Delta t_{k+1} - \Delta t_k) & R_{X_{k+1}X_{k+1}}(0) & \cdots & R_{X_{k+1}X_l}(\Delta t_{k+1} - \Delta t_l) \\ \vdots & \vdots & \vdots & \vdots \\ R_{X_lX_k}(\Delta t_l - \Delta t_k) & R_{X_lX_{k+1}}(\Delta t_l - \Delta t_{k+1}) & \cdots & R_{X_iX_l}(0) \end{bmatrix}. \tag{19}$$

The cross-correlation matrix between $\mathbf{X}_v$ and $\mathbf{Y}_v$ at time lag zero is given by

$$\mathbf{R}_{\mathbf{X}_v\mathbf{Y}_v} = E[\mathbf{X}_v(t)\mathbf{Y}_v^{\mathrm{T}}(t)]$$

$$= \begin{bmatrix} R_{X_1X_k}(\tau - \Delta t_k) & R_{X_1X_{k+1}}(\tau - \Delta t_{k+1}) & \cdots & R_{X_1X_l}(\tau - \Delta t_l) \\ R_{X_2X_k}(\tau - \Delta t_k) & R_{X_2X_k{}^{+1}}(\tau - \Delta t_{k+1}) & \cdots & R_{X_2X_l}(\tau - \Delta t_l) \\ \vdots & \vdots & \vdots & \vdots \\ R_{X_nX_k}(\tau - \Delta t_k) & R_{X_nX_{k+1}}(\tau - \Delta t_{k+1}) & \cdots & R_{X_nX_l}(\tau - \Delta t_l) \end{bmatrix} \tag{20}$$

The vector triggering condition is now defined as a vector level crossing triggering condition:

$$T^L_{\mathbf{Y}_v(t+\Delta\mathbf{t})} = \{X_k(t + \Delta t_k) = y_k, \ldots, X_l(t + \Delta t) = y_l\}. \tag{21}$$

The name vector level crossing triggering condition is used because a discrete-time measurement will never fulfill the above conditions. Instead the condition is fulfilled when all l measurements crosses the lines y_i from either above or below. Because $\mathbf{X}(t)$ has been assumed to have, a zero mean, the conditional mean value can be calculated from the standard results for zero mean Gaussian processes (see reference [24]),

$$E[\mathbf{X}_v | T^L_{\mathbf{Y}_v(t+\Delta\mathbf{t})}] = E[\mathbf{X}_v | \mathbf{Y}_v = \mathbf{y}_v] = \mathbf{R}_{\mathbf{X}_v\mathbf{Y}_v} \cdot \mathbf{R}^{-1}_{\mathbf{Y}_v\mathbf{Y}_v} \cdot \mathbf{y}_v, \tag{22}$$

where a triggering level vector, $\tilde{\mathbf{a}}$, is defined as

$$\tilde{\mathbf{a}} = \mathbf{R}^{-1}_{\mathbf{Y}_v\mathbf{Y}_v} \cdot \mathbf{y}_v, \quad \tilde{\mathbf{a}} = [\tilde{a}_k\ \tilde{a}_{k+1}\ \ldots\ \tilde{a}_l]^{\mathrm{T}}, \quad \mathbf{y}_v = [\tilde{y}_k\ \tilde{y}_{k+1}\ \ldots\ \tilde{y}_l]^{\mathrm{T}}, \tag{23}$$

and $\tilde{y}_k$ is the chosen triggering level for the kth measurement. The VRD functions can be rewritten by using equation (23):

$$\mathbf{D}^v_{\mathbf{X}}(\tau + \Delta\mathbf{t}) = E[\mathbf{X}_v | T^L_{\mathbf{Y}_v(t+\Delta\mathbf{t})}] = \mathbf{R}_{\mathbf{X}_v\mathbf{Y}_v} \cdot \tilde{\mathbf{a}}. \tag{24}$$

The VRD functions are thereby given as a sum of correlation functions determined solely from the formulation and size of the vector triggering condition:

$$\mathbf{D}^v_{\mathbf{X}}(\tau) = \mathbf{R}_{X_k}(\tau - \Delta t_k) \cdot \tilde{a}_k + \mathbf{R}_{X_{k+1}}(\tau - \Delta t_{k+1}) \cdot \tilde{a}_{k+1} + \cdots + \mathbf{R}_{X_l}(\tau - \Delta t_l) \cdot \tilde{a}_l. \tag{25}$$

Notice that if $k = l$ and $\Delta t_k = 0$ in equation (21), the traditional RD formulation for the level triggering condition is obtained

$$D_{X_1X_1}(\tau) = R_{X_1X_1}(\tau) \cdot \tilde{a}_1 = \frac{R_{X_1X_1}(\tau)}{\sigma^2_{X_1}} \cdot a_1 \,. \tag{26}$$

The probability that $\mathbf{Y}_v = \mathbf{y}_v$ occurs is very small. This means that the expected number of triggering points can easily be too small to achieve a VRD function which has converged acceptably. Instead, a vector triggering condition where each triggering measurement must be in between two values is formulated. This will increase the number of triggering points. The condition will be denoted as the vector positive point triggering condition:

$$T^p_{\mathbf{Y}_v(t+\Delta\mathbf{t})} = \{a_k \leqslant X_k(t + \Delta t_k) \leqslant b_k, \ldots, a_l \leqslant X_l(t + \Delta t_l) \leqslant b_l\}. \tag{27}$$

All sets of a_i and b_i must have the same sign. The maximum number of triggering points is always obtained by choosing $\mathbf{a} = 0$ and $\mathbf{b} = |\infty|$. In order to link this triggering condition with the results from equations (19) and (20) the result in equation (24) are used

$$\begin{aligned}
\mathbf{D}_{\mathbf{X}}(\tau + \Delta\mathbf{t}) &= E[\mathbf{X}_v | \, T^P_{Y_u(t+\Delta\mathbf{t})}] = E[\mathbf{X}_v | \mathbf{a} < \mathbf{Y}_v \leqslant \mathbf{b}] \\
&= \int_{-\infty}^{\infty} \mathbf{x}_v p_{\mathbf{X}_v | T^p_{\mathbf{Y}_v(t+\Delta\mathbf{t})}}(\mathbf{x}_v | \, T^P_{\mathbf{y}_v(t+\Delta\mathbf{t})}) \, \mathrm{d}\mathbf{x}_v \\
&= \frac{1}{k_1} \int_{\mathbf{a}}^{b} \int_{-\infty}^{\infty} \mathbf{x}_v p_{\mathbf{X}_v | \mathbf{Y}_v(\mathbf{x}_v | \mathbf{y}_v)} \, \mathrm{d}_{\mathbf{x}_v} p_{\mathbf{Y}_v}(\mathbf{y}_v) \, \mathrm{d}\mathbf{y}_v, \\
&= \mathbf{R}_{\mathbf{X}_v\mathbf{Y}_v} \cdot \mathbf{R}^{-1}_{\mathbf{Y}_v\mathbf{Y}_v} \cdot \frac{1}{k_1} \cdot \int_{\mathbf{a}}^{\mathbf{b}} \mathbf{y}_v p_{\mathbf{Y}_v}(\mathbf{y}_v) \, \mathrm{d}\mathbf{y}_v, \\
&= \mathbf{R}_{\mathbf{X}_v\mathbf{Y}_v} \cdot \tilde{\mathbf{a}}.
\end{aligned} \tag{28}$$

Here p is the probability density function and the triggering level $\tilde{\mathbf{a}}$ is now defined as

$$\tilde{\mathbf{a}} = \frac{\mathbf{R}^{-1}_{\mathbf{Y}_v\mathbf{Y}_v}}{k_1} \int_{\mathbf{a}}^{\mathbf{b}} \mathbf{y}_v \cdot p(\mathbf{y}_v) \, \mathrm{d}y_v, \quad k_1 = \int_{\mathbf{a}}^{\mathbf{b}} p_{\mathbf{Y}_v}(\mathbf{y}_v) \, \mathrm{d}\mathbf{y}_v. \tag{29}$$

So the vector positive point triggering condition gives results equivalent to the vector level crossing triggering condition:

$$\mathbf{D}^v_{\mathbf{X}}(\tau) = \mathbf{R}_{X_k}(\tau - \Delta t_k) \cdot \tilde{a}_k + \mathbf{R}_{X_{k+1}}(\tau - \Delta t_{k+1}) \cdot \tilde{a}_{k+1} + \cdots + \mathbf{R}_{X_l}(\tau - \Delta t_l) \cdot \tilde{a}_l. \tag{30}$$

Only the weights, $\tilde{a}_i$, of the correlation functions have changed. In partice, only the vector positive point triggering condition is of interest, since this is the only triggering condition which results in a reasonable number of triggering points.

In conclusion, the VRD functions are a sum of a number of correlation functions corresponding to the size of the vector condition. The result in equation (30) is important since the modal parameters can be extracted from the VRD functions by using the methods mentioned in section 2. The advantage of the VRD technique is

that by performing only, a single set of VRD functions, information from several correlation functions is available. For example for the FFT-IFFT approach a corresponding algorithm is not formulated.

A single problem arises when methods developed to extract modal parameters from free decays are used to extract modal parameters from VRD functions. These methods can deal only with positive time lag correlation functions. The *decays* should dissipate with increasing time lags. This is not the case for the part of the correlation functions which has negative time lags. This also means that the VRD functions cannot be used directly as input to the ITD or PTD methods. First of all, only the part of the VRD functions with $\tau \geqslant 0$ can be used. Furthermore, a number of points corresponding to $\max(\Delta t_i)$ should be removed from all functions. Otherwise, a part from the correlation functions with negative time lags is used in the modal parameter extraction procedure, see equation (30). This can result in highly erroneous damping ratios.

3.1. CHOICE OF TIME SHIFTS

Another problem is to choose the time shifts $\Delta t_k, \Delta t_{k+1}, \ldots, \Delta t_l$ so that the maximum number of triggering points is obtained. The obvious possibility is to estimate a column in the correlation matrix at several positive as well as negative time points using the traditional RD technique. To obtain the maximum number of triggering points for the VRD technique, the time shifts Δt_i can be chosen from

$$\max(|D_{X_iX_j}(\tau)|) \Rightarrow \Delta t_i = \tau. \tag{31}$$

Notice that the time shift corresponding to $i = j$ will always be $\Delta t_i = 0$ which is always the time lag with maximum value for the autocorrelation functions of a stationary process. If $D_{X_iX_j}(\Delta t_i)$ is negative, the triggering levels, a_i and b_i should also be negative.

3.2. QUALITY ASSESSMENT

In application of the VRD technique, it is convenient to have a standard procedure to assess the quality of the estimated VRD functions. Theoretically, the absolute value of the VRD functions estimated by using the following two triggering conditions should be exactly equal due to symmetry:

$$T^{P,1}_{\mathbf{Y}_v(t+\Delta\mathbf{t})} = \{a_k \leqslant X_k(t + \Delta t_k) \leqslant b_k, \ldots, a_l \leqslant X_l(t + \Delta t_l) \leqslant b_l\}, \tag{32}$$

$$T^{P,2}_{\mathbf{Y}_v(t+\Delta\mathbf{t})} = \{ -b_k \leqslant X_k(t + \Delta t_k) \leqslant -a_k, \ldots, -b_l \leqslant X_l(t + \Delta t_l) \leqslant -a_l\}. \tag{33}$$

with the VRD functions denoted as $D^{v,1}_{\mathbf{XX}_{kl}}(\tau)$ and $D^{v,2}_{\mathbf{XX}_{kl}}(\tau)$, estimated by using $T^{P,1}_{\mathbf{Y}_v(t+\Delta\mathbf{t})}$ and $T^{P,2}_{\mathbf{Y}_v(t+\Delta\mathbf{t})}$ from equations (32) and (33), average and error VRD functions can be estimated as

$$\hat{\mathbf{D}}^{average}_{\mathbf{XX}_{k,l}}(\tau) = (\hat{\mathbf{D}}^{v,1}_{\mathbf{XX}_{k,l}}(\tau) - \hat{\mathbf{D}}^{v,2}_{\mathbf{XX}_{k,l}}(\tau))/2, \tag{34}$$

$$\hat{\mathbf{D}}^{error}_{\mathbf{XX}_{k,l}}(\tau) = (\hat{\mathbf{D}}^{v,1}_{\mathbf{XX}_{k,l}}(\tau) + \hat{\mathbf{D}}^{v,2}_{\mathbf{XX}_{k,l}}(\tau))/2, \tag{35}$$

By plotting the average and corresponding error VRD functions, the quality of the VRD function can be validated. Alternatively, the root mean square of the error VRD functions divided by the root mean square of the average VRD functions can be used as a single measure of the quality of each VRD function.

3.3. EXPECTED NUMBER OF TRIGGERING POINTS

Due to the link between the VRD functions and the correlation functions, the expected number of triggering points can be predicted by

$$N = \frac{N_{Time}}{f_s} \int_{\mathbf{a}}^{\mathbf{b}} p_{\mathbf{y}_v}(\mathbf{y}_v)\, \mathrm{d}\mathbf{y}_v, \tag{36}$$

where N_{Time} is the number of points in the measurements minus the number of points in the VRD functions and f_s is the sampling frequency.

The prediction of the number of triggering points can be used in simulation studies for exact prediction or in a real situation by choosing a proper correlation matrix for $\mathbf{Y}_v$.

4. SIMULATION STUDY

The purpose of this example is to illustrate the theoretical developments in section 3. A simple 3DOF linear lumped mass parameter system is considered. The modal parameters of the system are given in Table 1.

The mode shapes are approximately in or out of phase. The 3DOF system is loaded by uncorrelated white noise at each mass and 20 000 points are simulated at a sampling interval of 0·045 s. Figure 2 shows the theoretical correlation matrix of the response for positive time lags and Figure 3 shows the corresponding spectral densities.

As seen from Figures 2 and 3, not all modes are well represented in all of the three columns of the correlation matrix. This means that it will be very difficult to estimate all modes from a single or two correlation columns.

In order to estimate a set of VRD functions, an initial estimate of the first column of the correlation matrix is performed using the traditional RD technique (level crossing triggering). The estimation time in CPU-time was 0·05 s and the result is shown in Figure 4.

TABLE 1

Modal parameters of 3DOF system

f(Hz)	ζ (%)	$\lvert\Phi_1\rvert$	$\lvert\Phi_2\rvert$	$\lvert\Phi_3\rvert$
1·00	2·00	1·000	0·084	0·006
3·00	2·00	− 0·085	1·000	0·110
9·00	2·00	0·006	− 0·110	1·000

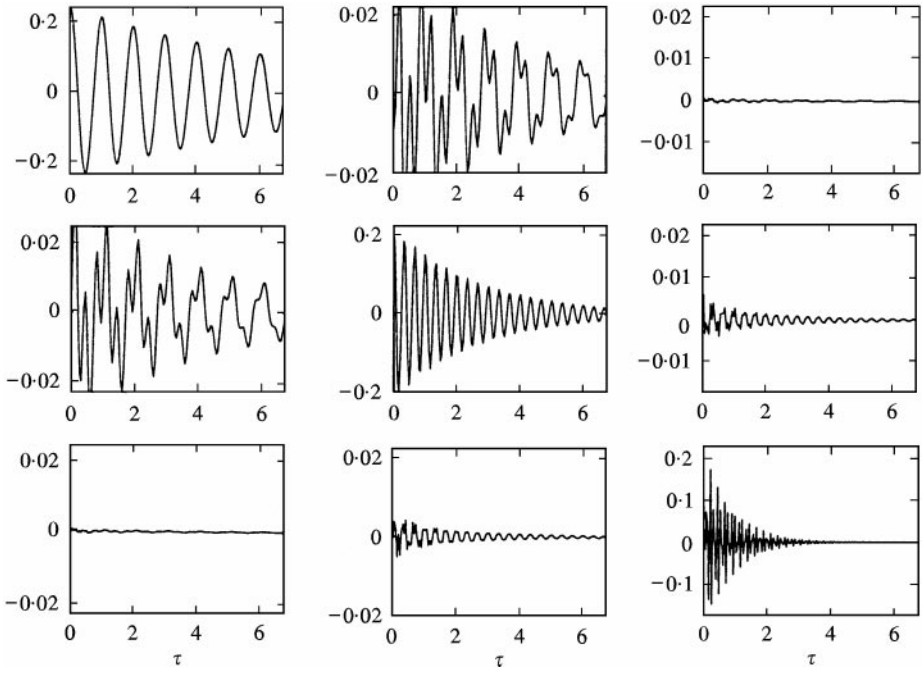

Figure 2. Correlation functions of the response of the 3DOF system.

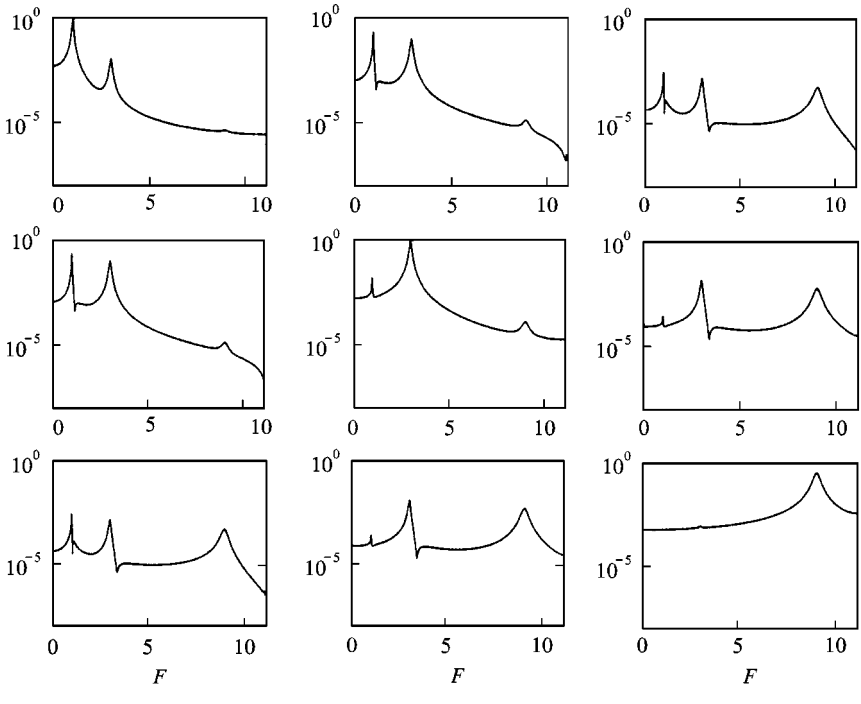

Figure 3. Spectral densities (absolute values) of the response of the 3DOF system.

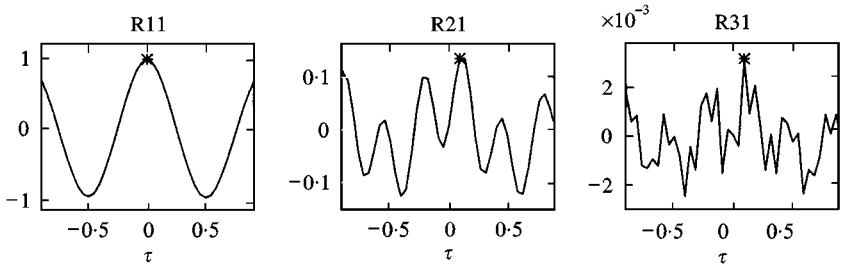

Figure 4. Initial estimate of the first column of correlation functions for decision of time shifts.

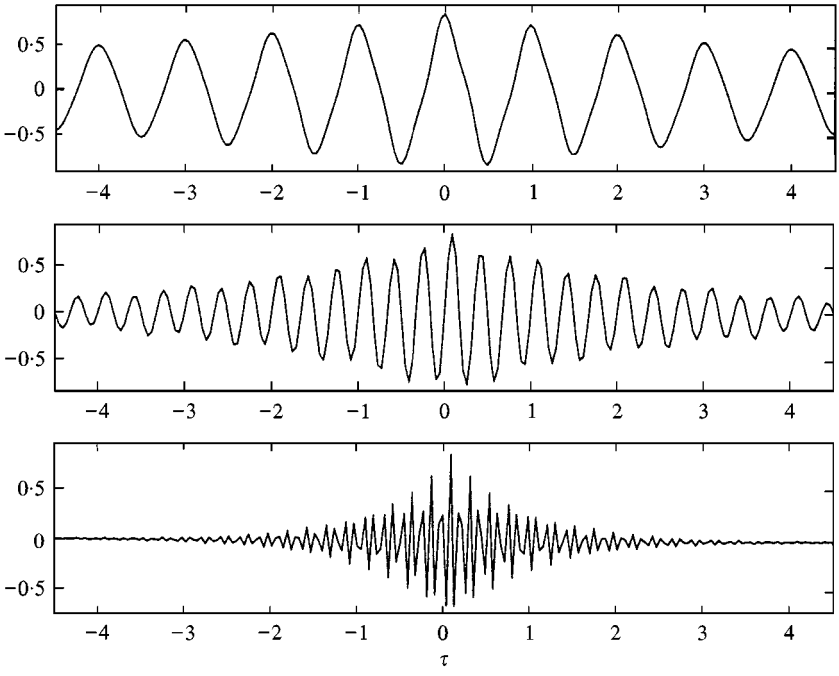

Figure 5. Theoretical VRD functions for positive and negative time lags.

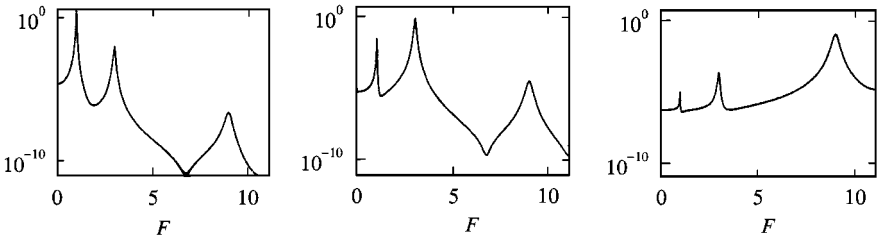

Figure 6. Fourier transform of the VRD functions in Figure 4 (absolute values).

The theoretical VRD functions using the optimal time shifts indicated by * in Figure 4 are shown in Figure 5, and the Fourier transform of the theoretical VRD functions is shown in Figure 6. The theoretical VRD functions can be predicted from the correlation functions of the linear system loaded by the white noise and the results derived in section 3.

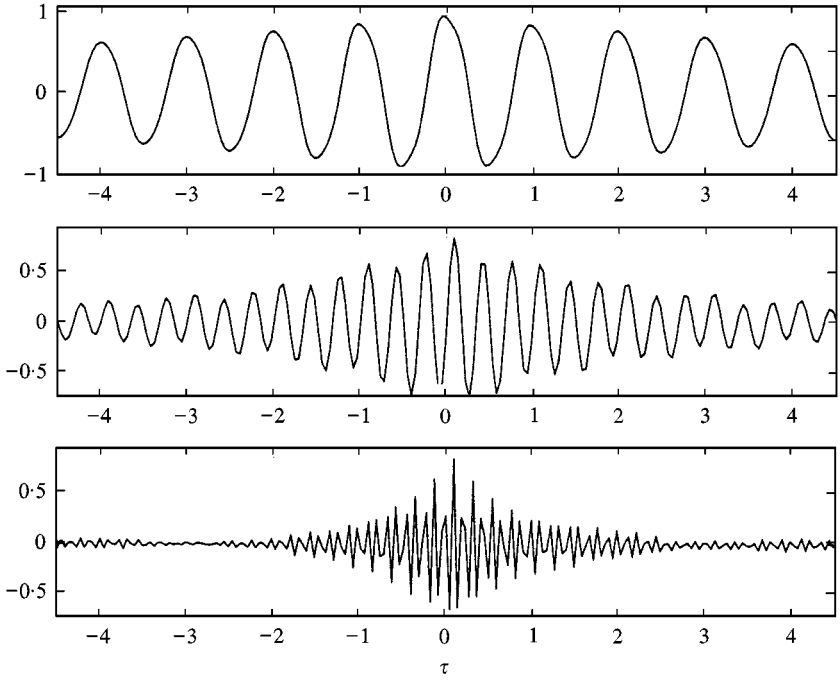

Figure 7. Estimated VRD functions for positive and negative time lags.

Figures 5 and 6 show that the VRD functions contain more information about the 3 modes than the columns of the correlation functions. An estimate of the VRD functions from the simulated response is shown in Figure 7.

The number of triggering points was 1440 and the expected number of triggering points was 1600. The CPU estimation time of the VRD functions was 0·33 s. For comparison the CPU estimation time of the full RD matrix using the traditional RD technique was 2·80 s and the number of triggering points was approximately 3000 for each column in the correlation matrix. The triggering level were $[a_1 \ a_2] = [\sigma_X \ \infty]$. Figure 8 shows the average and error VRD functions as suggested in section 3.2.

The dotted lines show that the error increases with the distance from time lag zero. For the VRD function shown in the third sub plot, it is seen that for $|\tau| > 2$ s the VRD functions become too uncertain for extraction of modal parameters.

5. CONCLUSION

The Vector Random Decrement technique is originally interpreted as a method for transforming ambient responses into free decays of linear structures. This paper extends the theoretical background of the VRD functions by considering zero mean Gaussian processes. The processes could for example be the response of linear structures loaded by filtered white noise. It is shown that the VRD function is a sum of the correlation functions of the Gaussian processes. The mathematical modes of

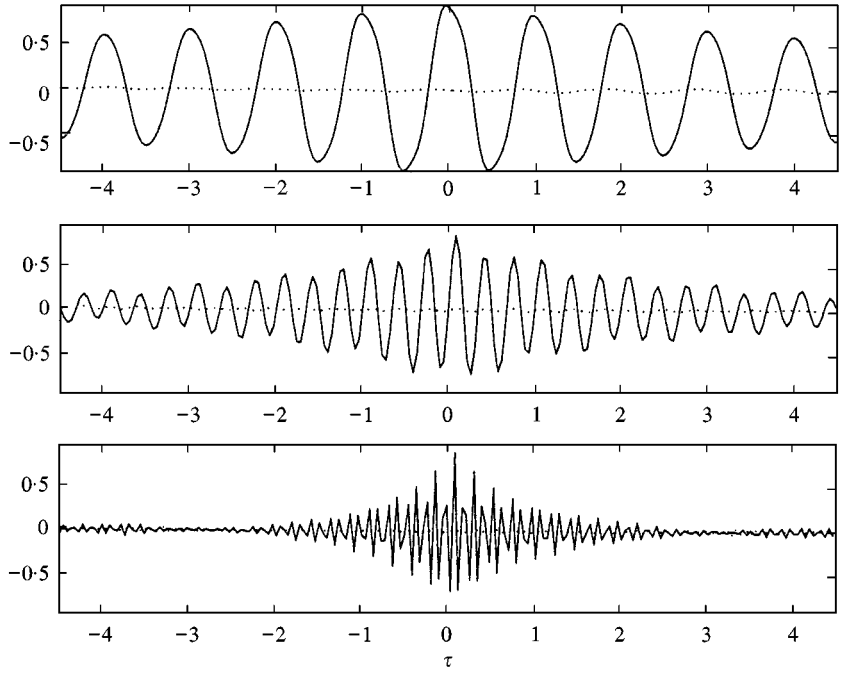

Figure 8. Average and error VRD functions for positive and negative time lags.

the shaping filter and the physical modes of the linear system are represented in the correlation functions. Therefore, the modes of both the linear system and the shaping filter can be identified from the VRD functions. The VRD functions depend on the size of the vector triggering condition and the time shifts used for the choice of triggering condition. This result makes the theory of the VRD technique as well developed as the theory of the RD technique.

A simulation study of a 3DOF system has been presented. The VRD technique is illustrated and it is shown that the VRD functions may contain as much information about the modes as the full correlation matrix of the processes. Furthermore, the estimtion time of the VRD functions is much lower than the estimation time of the full correlation matrix using the traditional RD technique (0·50–2·80 s in CPU time).

The VRD technique can be an excellent choice of algorithm for the analysis of data, where a large number of measurements is collected. It then becomes very tedious to estimate the full correlation matrix using an FFT algorithm or the traditional RD technique. By using the VRD technique, the information from the full correlation can be compressed in the VRD functions at a faster estimation time.

ACKNOWLEDGMENTS

Financial support from the Danish Technical Research Council is gratefully acknowledged.

REFERENCES

1. S. R. Ibrahim, R. Brincker and J. C. Asmussen 1996 *Proceedings* 14*th International Modal Analysis Conference* I, 446–452. Modal Parameter identification from responses of general unknown random inputs.
2. J. C. Asmussen 1997 *Ph.D.-Thesis Aalborg University*, *Denmark*. Modal analysis based on the random decrement technique—applications to civil engineering structures.
3. C. R. Farrar and G. H. James III 1997 *Journal of Sound Vibration* **205**, 1–18. System identification from ambient vibration measurements on a bridge.
4. G. H. James III, T. G. Carne and J. P. Lauffer 1995 *Modal Analysis* **10**, 260–277. The natural excitation technique (NEXT) for modal parameter extraction from operating structures.
5. J. S. Bendat and A. G. Piersol 1986 *Random Data—Analysis and Measurement Procedures*. New York: Wiley, ISBN 0-471-04000-2.
6. A. Fasana, L. Garibaldi, M. Ruzzen and D. Sabia 1997 *Proceedings of the* 15*th International Modal Analysis Conference*, Vol. I, 293–300. Analysis of a motorway bridge under random traffic excitation.
7. M. J. Desforges, J. E. Cooper and J. R. Wright 1995 *Mechanical Systems and Signal Processing* **9**, 169–186. Spectral and modal parameter estimation from output-only measurements.
8. M. Ruzzene, A. Fasana, L. Garibaldi and B. Piombo 1997 *Mechanical Systems and Signal Processing* **11**, 207–218. Natural frequencies and dampings identification using wavelet transform: application to real data.
9. J. C. Asmussen, S. R. Ibrahim and R. Brincker 1996 *Proceedings of the* 14*th International Modal Analysis Conference*, Vol. I, 453–458. Random decrement and regression analysis of traffic responses of bridges.
10. J. C. Asmussen, S. R. Ibrahim and R. Brincker 1998 *Proceedings of the* 16*th International Modal Analysis Conference*. Random decrement: identification of structures subjected to ambient excitation.
11. J. C. Asmussen A. Rytter and R. Brincker 1998 *Proceedings of the* 16*th International Modal Analysis Conference*. Ambient testing of the Vestvej Bridge.
12. H. A. Cole 1968 *AIAA Paper No*. 68-288. On-the-line analysis of random vibrations.
13. H. A. Cole 1971 *United States Patent No*. 3, 620,069. Method and apparatus for measuring the damping characteristics of a structure.
14. H. A. Cole 1971 NASA TMX-62,041. Failure detection of a space shuttle wing by random decrement.
15. H. A. Cole 1973 NASA CR-2205. On-line failure detection and damping measurements of aerospace structures by random decrement signature.
16. S. R. Ibrahim 1977, *Journal of Spacecraft and Rockets* **14**, 696–700. Random decrement technique for modal identification of structures.
17. S. R. Ibrahim 1977 *AIAA Paper*, *Vol*. 77, 1–9. The use of random decrement technique for identification of structures modes of vibration.
18. J. K. Vandiver, A. B. Dunwoody, R. B. Campbell and M. F. Cook 1982 *Journal of Mechanical Design* **104**, 307–313. A mathematical basis for the random decrement vibration signature analysis technique.
19. R. Brincker, S. Krenk, P. H. Kirkegaard and A. Rytter 1992 *Bygningsstatiske Meddelelser*, **63**, 1–38. Identification of dynamical properties from correlation function estimates.
20. J. C. Asmussen and R. Brincker 1996 *Proceedings of the ISMA*21*—Noise and Vibration Engineering*, Vol. II, 1215–1224. Estimation of correlation functions by random decrement.
21. S. R. Ibrahim, J. C. Asmussen, R. Brincker 1998 *Accepted ASME Journal of Vibration and Acoustics*. Vector triggering random decrement for high identification accuracy.

22. S.R. Ibrahim, J. C. Asmussen, and R. Brincker 1997 *Proceedings of the* 15*th International Modal Analysis Conference*, Vol. I, 502–510. Theory of the vector random decrement technique.
23. J. C. Asmussen S. R. Ibrahim, and R. Brincker 1997 *Proceedings of the* 15*th International Modal Analysis Conference*, Vol. I, 502–510. Application of the vector triggering random decrement technique.
24. J. L. Melsa and A. P. Sage 1973 *An Introduction to Probability and Stochastic Processes.* Englewood Cliffs, NJ: Prentice-Hall, Inc. ISBN: 0-13-034850-3.